Journal of Fluorine Chemistry 131 (2010) 975–981

Contents lists available at ScienceDirect

Journal of Fluorine Chemistry

journal homepage: www.elsevier.com/locate/fluor

Investigation of ion-pairing phenomenon in BaF_2 aqueous solution: Experimental and theoretical studies

B. Sohrabi [a,*], M. Aghaie [b], A. Aliabadi [b]

[a] Department of chemistry, Surface Chemistry Research Laboratory, Iran University of Science and Technology, P.O. Box 16765-163, Tehran, Iran
[b] Faculty of chemistry, North Tehran branch, Islamic Azad University, Tehran, Iran

ARTICLE INFO

Article history:
Received 10 November 2009
Received in revised form 5 July 2010
Accepted 7 July 2010
Available online 14 July 2010

Keywords:
Contact ion-pair
Ion association
NMR spectroscopy
Ab initio
DFT
NQR spectroscopy
HOMO
LUMO

ABSTRACT

The ion-pair association constant values, related to the reaction $Ba^{2+} + F^- \leftrightarrows [BaF]^+$, are determined by means of NMR spectroscopy. The values for thermodynamic functions of the ion-pairing process are calculated on the basis of the NMR results. In addition, the association entropy has been found to be dependent on temperature. Comparing the experimental data and Fuoss theory, it is found that $[BaF]^+$ contact ion-pair is formed in the BaF_2 aqueous solution. Also, hydration of barium-fluoride ion-pair is investigated by the DFT method. The hydration number of barium-fluoride ion-pair is determined by comparing the experimental and theoretical results. The effect of number of water molecules on the properties of ion-pairs is investigated by determining NQR and NMR parameters. Also, the relation between the chemical shifts and the energy gap between the highest occupied molecular orbital (HOMO) and low-lying virtual molecular orbital (LUMO) is investigated.

1. Introduction

In the Debye–Hückel theory, it is assumed that strong electrolytes completely dissociate in aqueous solution [1]. However, there is also much evidence to show that cations and anions in solution can associate to form ion-pairs, as a result of strong electrostatic attraction. In ionic compounds, the separation to ions is complete. However, if ions associate in solution, the dissociation is not complete. Small ion dimensions, high ion valence, and small solvent dielectric constants are conducive to ion-pair formation.

Hydration of ion-pairs is an essential process in the solvation of ionic crystals into water, chemical reactions in aqueous solution, and stability and functionality of biological systems [2–4]. Solvation effects can profoundly alter chemical and physical interactions.

The investigations show that dissolved ions in water have "structure making" or "structure breaking" effects on water, depending on the ionic size and whether they are cations or anions [5]. For example, halide ions larger than Cl^-, i.e. Br^- and I^-, are regarded as water structure breakers, while smaller ions such as F^- are regarded as water structure makers. Yet it could equally be argued that a smaller ion, with its much greater local charge density, would be more likely to pull the water away from its hydrogen bonded configuration in the liquid than a larger ion, thus breaking the water structure [6,7]. Hribar et al. concluded that "small ions have high charge densities, so they cause strong electrostatic ordering of nearby water molecules, breaking hydrogen bonds" [7]. In other words, an ion which breaks water hydrogen bonds is regarded as a structure maker.

The ion-pairs were classified on the basis of mutual geometry of the ions and the solvent according to: (1) solvent-separated ion-pairs, (2) solvent-shared ion-pairs and (3) contact ion-pairs [8].

Several methods of studying ion-pairing including conductivity methods [9–15], ion-selective electrode potentiometry [16], gravimetric, solvent evaporation [17], NMR spectroscopy [18–22], and theoretical modeling [23–26] have been used to probe the phenomenon of ion association in both aqueous and non-aqueous solvents. Theoretical methods like DFT assume some structures in the solution and only a correct assumption leads to a theoretical result that agrees with experimental results. Thus, such agreement indicates indirectly the structure of the molecules. For example, the experimental and theoretical studies have been shown that Mg^{2+} is coordinated by six water molecules in an octahedral arrangement [27]. Also, the DFT and experimental ^{19}F NMR chemical shifts for sulfur-containing compounds have been shown

* Corresponding author. Fax: +98 2177491204.
E-mail addresses: sohrabi_b@yahoo.com, sohrabi_b@iust.ac.ir (B. Sohrabi).

0022-1139/$ – see front matter © 2010 Elsevier B.V. All rights reserved.
doi:10.1016/j.jfluchem.2010.07.001

that the fluorine atom is attached to a four and a six-coordinated sulfur atom [28]. Also, the experimental methods as extended-X-ray adsorption fine structure spectroscopy and large-angle X-ray scattering and theoretical methods such as molecular dynamic method have been used for determining of hydration number of Ca^{2+} in dilute $CaCl_2$ solution [29,30].

The phenomenon of ion association from the various aspects, e.g. plating and holding of tertiary structure of enzymes and proteins [31], maintaining the micelle stability [32], lowering the electric conductivity in Li-ion battery electrolytes, is of great interest.

Since careful analysis of NMR spectra for a nucleus exchanging among different environments yields information about the exchange process [33,34], for processes involving ion solvation, one can investigate the NMR spectroscopy of the solvent such as water [35]. But NMR investigation of the ion also provides direct evidence of exchange. ^{19}F NMR studies of aqueous salt solutions at room temperature show a significant variation in the NMR chemical shifts with concentration.

Choppin and Majer previously calculated thermodynamic parameters of the alkaline earth monofluorides in ionic strength 1 M. The investigations showed that the formation constant of ion-pair is small in high ionic strength [36,37].

In this study, we report the temperature and concentration dependence of ^{19}F NMR shifts of BaF_2 solutions, from which we have determined equilibrium constants as a function of temperature, the free energy, enthalpy and entropy of formation of the ion-pair in aqueous solution.

We studied the hydration process of $[BaF]^+$ in water by ab initio method and compared the results of theory and experiment to determine hydration number of $[BaF]^+$. Also, we investigated the effect of the number of water molecules present on the ion-pair properties by determining the NQR and NMR parameters.

2. Results and discussion

2.1. Ion-pairing in aqueous solution of BaF_2

Using NMR spectroscopy, we focused on the following ion-pairing:

$$Ba^{2+} + F^- \leftrightarrows [BaF]^+ : \quad K = \frac{a_{[BaF]^+}}{a_{Ba^{2+}} a_{F^-}} \tag{1}$$

Careful analysis of NMR spectra for a nucleus exchanging among different environments yields information about the exchange process. For process involving ion solvation, one can investigate the NMR spectroscopy of the solvent such as water [18]. In addition, comparing experimental data to Fuoss theory leads to evaluate ion association phenomenon and the type of ion-pair [1,8].

NMR investigation of the ion provides direct evidence of exchange ^{19}F. Also, NMR studies of the aqueous salt solutions at room temperature show a significant variation in the NMR chemical shifts with concentration. In this study, we report the temperature and concentration dependence of ^{19}F NMR shifts of BaF_2 solutions from which we determined equilibrium constants of formation of $[BaF]^+$ as a function of temperature, and then we calculated the enthalpy and the entropy of ion-pair formation in aqueous solution.

The NMR spectra of the fluoride ion in BaF_2 solution at different concentrations and temperatures consist of a single sharp resonance. Fig. 1 shows that chemical shift is strongly temperature-dependent at constant concentration. The NMR method enables us to study the phenomenon of ion-pairing. When the exchange of the F^- ion between the free state and ion-pair state (according to reaction 1) is fast, dependence of chemical shifts on

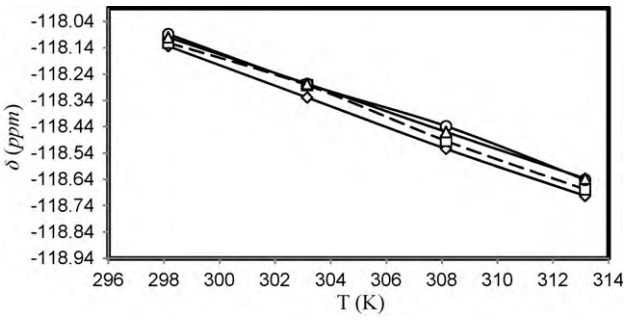

Fig. 1. Variation in chemical shift as a function of temperature at constant concentration: 0.0018 (◇), 0.0035 (△), 0.0038(○), 0.0043 (□). All concentrations are in mol L^{-1}.

the concentration of the F^- ion can be treated as follows [18–20,38]:

$$\delta = \alpha\delta_{free} + (1-\alpha)\delta_{ion\text{-}pair} \tag{2}$$

where δ_{free} and $\delta_{ion\text{-}pair}$ are the chemical shifts of the F^- ion in the free and ion-pair states, respectively, and α is the fraction of the total F^- ions that are free in solution. The inverse of the exchange rate, τ, (mean lifetime) is given by [18]:

$$\tau = \frac{\tau_{free}\tau_{ion\text{-}pair}}{\tau_{free} + \tau_{ion\text{-}pair}} \tag{3}$$

where τ_{free} and $\tau_{ion\text{-}pair}$ are the lifetimes of the F^- ion in the free and ion-pair states, respectively.

It is obvious that there is a critical total concentration, M^*, below which ($\alpha = 1$) the ion-pair, $[BaF]^+$, is not formed, while above it ($\alpha < 1$), it is formed. Thus as an approximation, we may assume that:

$$\alpha = \frac{M^*}{M_{tot}} \tag{4}$$

where M_{tot} represents the total concentration (in mol L^{-1}) of BaF_2 in solution. Substituting Eq. (4) into Eq. (2) gives:

$$\delta = \left(\frac{M^*}{M_{tot}}\right)\delta_{free} + \left(1 - \frac{M^*}{M_{tot}}\right)\delta_{ion\text{-}pair} \tag{5}$$

or

$$\delta = \delta_{ion\text{-}pair} + \frac{M^*}{M_{tot}}(\delta_{free} - \delta_{ion\text{-}pair}) \tag{6}$$

Therefore, if $M_{tot} \le M^*$, then $\delta = \delta_{free}$ and $\alpha = 1$, but if $M_{tot} > M^*$, then $\delta = \delta_{ion\text{-}pair}$ (neglecting the second term in Eq. (6)) and $\alpha < 1$.

The overall plots of Eqs. (5) and (6) against the inverse of total concentration, M_{tot}^{-1}, of BaF_2 at a constant temperature gives two straight lines; one is horizontal, corresponding to the condition of $M_{tot} < M^*$ ($\delta = \delta_{free}$), and the other is sloped, corresponding to $M_{tot} > M^*$ (Fig. 2), while the intercept of the plot gives $\delta_{ion\text{-}pair}$. $\delta_{ion\text{-}pair}$ was determined using curve fitting the plot of δ versus M_{tot}^{-1} to linear equation and determining intercept of equation. It is clear that $\delta = \delta_{free}$, if the observed chemical shift is independent of M_{tot}.

Determining δ_{free} and $\delta_{ion\text{-}pair}$ by the procedure mentioned and substituting them into Eq. (2) yields the value of α. Thus we may calculate the stability constant for formation of $[BaF]^+$, as follows:

$$Ba^{2+}_{(aq)} + F^- \leftrightarrows [BaF]^+ : \quad K' = \frac{[BaF^+]}{\left[Ba^{2+}\right][F^-]}$$
$$M_{tot}(2\alpha - 1) \quad 2M_{tot}\alpha \quad 2M_{tot}(1-\alpha)$$
$$K' = \frac{(1-\alpha)}{M_{tot}(2\alpha^2 - \alpha)} \tag{7}$$

$$K = \frac{a_{BaF^+}}{a_{Ba^{2+}} a_{F^-}} \tag{8}$$

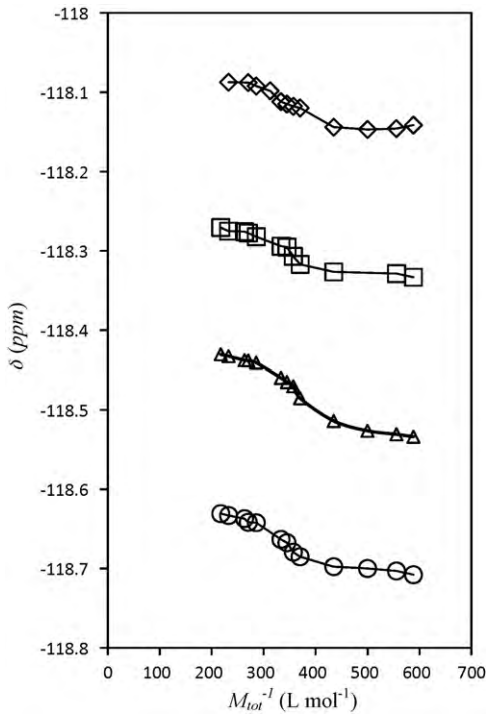

Fig. 2. Variation in chemical shift as a function of the inverse of total concentration of BaF_2 at: 298.15 K (◇), 303.15 K (△), 308.15 K (□), 313.15 K (○).

where $a_{BaF^+} = [BaF^+] f_{ion-pair}$; $a_{Ba^{2+}} = [Ba^{2+}] f_+$; $a_{F^-} = [F^-] f_-$; and f represents activity coefficient.

Individual ion activity can be calculated using extended Debye–Hückel equation [1].

$$\log f_i = -\frac{AZ_i^2\sqrt{I}}{1 + Ba'\sqrt{I}} + bI \quad (9)$$

where a' = 4 Å, B = 0.328 Å^{-1} and A = 0.509 for water in 25 °C and b is an empirical parameter (Appendix B).

As Eq. (7) shows, the association constant is concentration dependent. But the standard association constant, K, related to the ion-pair $[BaF]^+$, can be determined at intended temperature by the following linear extrapolation:

$$\log K = m - bI \quad (10)$$

where I is the total effective ionic strength in term of mol L^{-1} and b is an empirical parameter, and $m = \log K' + (4A\sqrt{I}/(1 + Ba'\sqrt{I}))$ (Appendix B). The least-square estimate of the intercept of the linear regression of m against I from Eq. (10) is $\log K$. The values of $\log K$ obtained by this approach are listed in Table 1.

On the other hand, one can estimate the association constant for various ion-pairs, on the basis of Fuoss theory, in dilute electrolyte solutions, as [1].

$$\ln K_f = \ln\left(\frac{4\pi a'^3 N}{3000}\right) + \frac{|Z_+Z_-|e^2}{a'DkT} \quad (11)$$

where N is the Avogadro constant, k is the Boltzmann constant, e is the elementary charge, a' is the distance of the closest approach between two ions, and D is dielectric constant of solvent. The values for $\log K_f$ calculated from Eq. (11) are also listed in Table 1. The concordance between the experimental and estimated values of $\log K_f$ is satisfactory.

Regarding the NMR results and Fuoss model, one can conclude that the degrees of dissociation and association constants of ion-pairing are temperature and dielectric constant dependent. Our experimental results show that $\ln K$ is a linear function of $1/DT$.

$$\ln K = A_1 + \frac{A_2}{DT} \quad (12)$$

where K represents the association constant of formation of $[BaF]^+$.

Our results were fitted by the Table Curve software on the basis of Eq. (12), and A_1 = 30.908 and $A_2 = -5.1962 \times 10^5$ K^{-1} were obtained with a coefficient of correspondence r = 0.998 and FitstdErr = 0.01028.

Table 1
Experimental and estimated (on the basis of Fuoss theory) values for $\log K$ and experimental thermodynamic functions (all in kcal/mol) for the formation of ion-pair at different temperatures.

Temperature (K)	D_w[a]	$\log K_f$	$\log K'$[b]	$\log K$[c]	ΔG_m^0	$T\Delta S_m^0$	ΔH_m^0
298.15	78.54	2.38	2.62	3.41	−4.60	34.40	29.80
303.15	76.76	2.40	2.59	3.26	−4.59	35.78	31.19
308.15	75.03	2.43	2.52	3.24	−4.58	37.22	32.64
313.15	73.34	2.47	2.45	3.21	−4.56	38.74	34.17

[a] D_w: water dielectric constant.
[b] K': concentration equilibrium constant.
[c] K: thermodynamic equilibrium constant.

2.2. The geometry of cyclic hydrated ion-pairs

The orientation of water molecules around $[BaF]^+$ ion-pair was investigated by DFT. The results show that the optimum structure for this ion-pair is cyclic, with Ba, F, O, and H_1 forming a nearly planar four-member ring (Fig. 3); H_2 is bent out of plane. A cyclic structure allows a water molecule to act as both donor and acceptor, simultaneously. Other structures in which water interacts with only the barium or the fluoride either lead to higher energy local minima or collapse to the cyclic structure.

Also, binding energies for the successive addition of water molecules were calculated. The metal–halogen bond was found to lengthen appreciably with increasing degree of solvation. We found binding energies for the addition water molecules in each step and the absolute values the binding energies would decrease (Table 2). The formation of ion-pair depends on steric self-repulsion, Van der Waals (vdW) attraction, and ion–dipole interactions of the system, and vdW attraction depends on ion size and charge. Therefore, with increase in the number of water molecules, due to increase in steric self-repulsion and ion–dipole interaction, barium-fluoride bond length increases. As the size of system grows, the charge distribution is increased and the water interaction with ion-pair is decreased. Table 2 shows that the hydrated ion-pair with seven water molecules is stable, because its binding energy is more negative than those of others. Fig. 4 shows the structure of this hydrated ion-pair.

We studied the strong interaction between the $[BaF]^+$ ion-pair and water molecules. Table 2 lists the total energies, aggregation energies, and geometrical parameters for the $[BaF]^+$ $(H2O)_n$

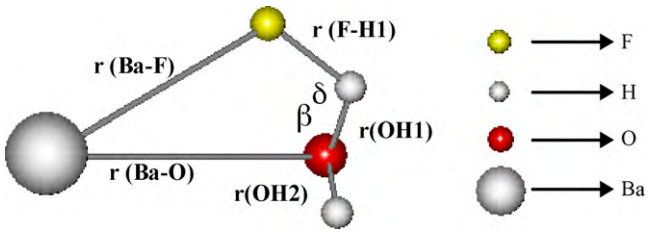

Fig. 3. Geometric parameters for cyclic BaF. H_2O cluster. Nine parameters were optimized. Shown in the figure are the bond lengths r(BaF), r(BaO), r(OH1), and r(OH2); the bond angles H1–O–Ba (β), F–H1–O (δ), F–Ba–O–H1 (γ) and F–H1–O–H2 (φ).

Table 2
Total energies, aggregation energies, and geometric parameters for $[BaF]^+(H_2O)_n$ clusters computed at the B3LYP level with LANL2DZ basis set.[a].

n	E	[b]ΔE	r(BaF)	r(BaO)	r(OH1)	r(OH2)	α	β	γ	φ
0	−125.2790	–	2.3069	–	–	–	–	–	–	–
1	−201.6328	37.9638	2.4141	2.5746	1.0355	0.9703	57.45	83.94	0.04	179.23
2	−277.9884	36.8334	2.5325	2.6105	1.0176	0.9712	56.66	87.43	0.04	179.87
3	−354.3448	36.3323	2.7409	2.6239	1.0106	0.9714	55.09	90.52	−0.09	−178.97
4	−430.8049	−28.7395	2.8121	2.6271	1.0160	0.9709	55.21	88.49	0.37	179.23
5	−507.2626	−27.2335	2.8340	2.6673	1.0060	0.9714	53.97	91.70	0.46	179.25
6	−583.7125	−22.3390	2.9976	2.6812	1.0159	0.9710	51.47	91.88	0.21	179.96
7	−660.1888	−38.9050	3.2186	2.6940	1.0190	0.9708	48.74	94.31	0.34	177.31
8	−736.6297	−16.6915	2.7643	2.6924	1.0063	0.9705	42.53	61.22	0.14	176.44
9	−813.0700	−16.3150	3.3101	2.6604	0.9800	0.9697	39.17	59.11	0.39	173.98
10	−889.5078	−14.7463	3.4707	2.6794	0.9917	0.9870	43.90	89.67	0.36	132.60

[a] Total energies are in hartree, energy differences are in kcal/mol, bond lengths are in Å, and angles are in degrees. See Fig. 1 for identification of parameters. Isolated water parameters are: $E = -76.4143$ hartree, r(OH) = 0.9768 Å and angle for water = 110.0450°.
[b] ΔE is $\Delta E = E_n - (E_{n-1} + E_{H_2O})$ for the equation: $[BaF]^+(H_2O)_{n-1} + H_2O \rightarrow [BaF]^+(H_2O)_n$.

clusters with no correction for basis set superposition error (BSSE). The results of Table 2 show that metal–halogen bond length increases with increase in the solvent-molecule number. Also, the results show that the r(Ba–O) and r(F–H_a) distances in $n = 1$ are 2.5746 and 1.5397 Å, respectively. These values are shorter than the sum of the ionic and vdW radii. Therefore, strong interactions exist between the $[BaF]^+$ ion-pair and water molecules.

2.3. Investigation of NQR parameters (EFG tensors) in $[BaF]^+(H_2O)_n$ clusters

Nuclear quadrupole coupling constant (NQCC), χ, and asymmetry parameter, η, for the ions were calculated for the ion-pairs. The effect of water molecule number on χ and η was studied. Fig. 5 shows the variations in these parameters with the number of water molecules for ^{135}Ba atom. The investigations show that χ is related to charge density on the atom and its symmetry. χ increases with increase in the charge density and decreases with decrease in the atom symmetry. According to Fig. 5, $[BaF]^+$ has axial symmetry in $n = 0$, and therefore, χ and η have the most and the least values, respectively. With increase in the number of water molecules and decrease in symmetry, χ decreases and η increases. The investigations show that χ and η have the most and the least values in $n = 0$, 3, 7, respectively. In other words, $[BaF]^+$ has the most symmetry with these number of water molecules. Therefore, with addition of water molecules, the charge density on the barium and fluorine atoms in $[BaF]^+$ increases but χ decreases due to the decrease in ion-pair symmetry.

2.4. Investigation of ^{19}F NMR parameters (chemical shielding tensors and chemical shifts) in $[BaF]^+(H_2O)_n$ clusters

In this part, the focus is on the effect of the number of water molecules on the ^{19}F NMR chemical shifts. To achieve this aim, DFT calculation was carried out at the B3LYP level of theory with LANL2DZ basis set for $[BaF]^+(H_2O)_n$ ($n = 0$–10) clusters. The calculated chemical shielding tensors were reported as chemical shielding principal components (σ_{ij}), chemical shielding isotropy (σ_{iso}), and chemical shielding anisotropy ($\Delta\sigma$) in Table 3. Also, ^{19}F NMR chemical shifts, δ, are tabulated in Table 3. Fig. 6 shows that F^- nucleus in $[BaF]^+$ ion-pair was deshielded with increase in the number of water molecules.

The ^{19}F NMR shift of the fluoride in $[BaF]^+$ ion-pair exhibits a large solvent dependence. According to the Ramsey theory of nuclear magnetic shielding, the shielding of a nucleus can be separated into two main contributions, the diamagnetic shielding (σ^d) and the paramagnetic shielding (σ^p) [39,40]. The diamagnetic shielding contribution describes the shielding of the nucleus from the external magnetic field by the surrounding electrons that induce a magnetic field opposite to the external one. The paramagnetic shielding contribution is a perturbation of the electron density currents that generally causes a decrease in the absolute shielding. In other words, the paramagnetic contribution, usually negative, is typically responsible for observed changes in chemical shifts for a given nucleus. Therefore, the ^{19}F NMR chemical shielding is dominated by paramagnetic shielding term, while the changes in the diamagnetic term are comparatively small. Fig. 6 shows that chemical shift of ^{19}F in $[BaF]^+$ increases with increase in the number of water molecules, since a solvent interaction of the fluoride atom in $[BaF]^+$ should result in an increased polarization of the charge distribution of F^- leading to an increased paramagnetic shift. According to Figs. 5 and 6 for $n = 8$, water molecules were asymmetrically added to second sheet, therefore the hydrated ion-pair symmetry and chemical shift decrease. In the result, the metal–halogen bond was found to shorten.

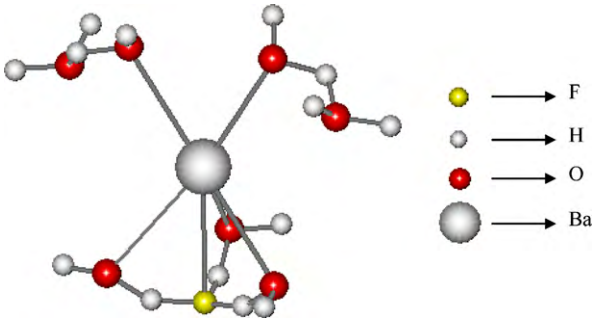

Fig. 4. The geometry optimizations structure $[BaF]^+(H_2O)_7$ obtained by DFT method.

Table 3
The calculated chemical shielding tensors of ^{19}F B3LYP/LANL2DZ in $[BaF]^+(H_2O)_n$ ion-pair.

n	σ_{11}[a]	σ_{22}	σ_{33}	σ_{iso}[b]	δ_{iso}[c]	$\Delta\sigma$
0	418.13	418.13	487.76	441.34	−248.64	69.62
1	332.53	360.52	484.09	392.38	−199.68	137.56
2	294.48	392.90	441.38	376.25	−183.55	97.68
3	344.90	345.82	359.48	380.07	−187.37	14.12
4	334.70	358.62	371.62	354.98	−162.28	24.96
5	328.40	346.08	361.09	345.19	−152.49	23.85
6	328.74	332.66	345.41	335.60	−142.90	14.71
7	308.66	315.99	321.93	315.53	−122.83	9.61
8	332.49	371.34	384.66	362.83	−170.13	32.74
9	301.29	322.42	439.47	354.39	−161.69	127.61
10	292.41	324.50	365.89	327.60	−134.90	57.44

[a] Calculated σ_{iso}, σ_{11}, σ_{22}, σ_{33} and $\Delta\sigma$ values in ppm.
[b] $\sigma_{iso}(r)$ 192.7 [31,32].
[c] Obtained δ_{iso} in this work is −117.90 ppm.

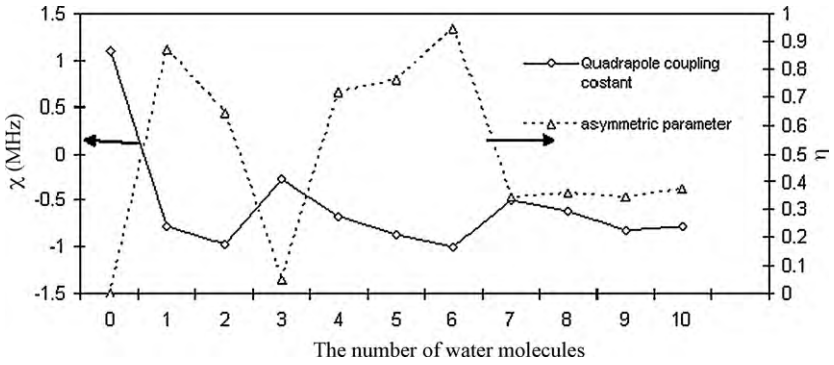

Fig. 5. The variation in nuclear quadrupole coupling constant (χ) and asymmetry parameter (η) versus the hydration number of water for ^{135}Ba atom.

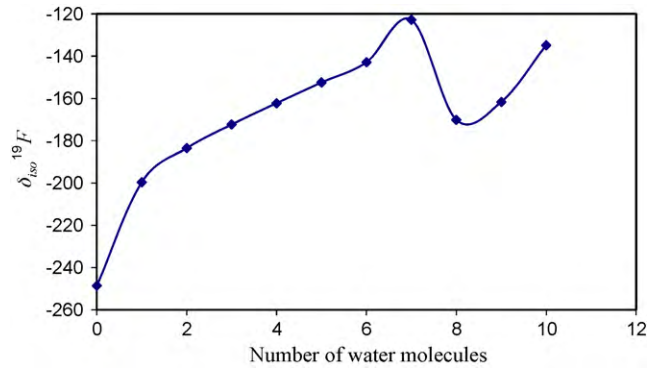

Fig. 6. The variations in ^{19}F NMR chemical shifts versus the number of water molecules. The chemical shifts obtained from $\delta_{iso} = \sigma_{iso,r} - \sigma_{iso,s}$. $CFCl_3$ with σ_{iso} of 192.7 ppm ^{19}F were chosen as the reference. σ_{iso} obtained by B3LYP/LANL2DZ level at 298.15 K.

The ^{19}F chemical shifts obtained by experimental and theoretical methods for $n = 7$ were −117.90 and −122.83 ppm, respectively. Therefore, this comparison shows that a good agreement exists between the experimental data and DFT calculations at $n = 7$.

Fig. 7 shows that the magnitude of chemical shift is directly related to the energy gap between the highest occupied molecular orbital (HOMO) and low-lying virtual molecular orbital (LUMO). Furthermore, the magnitude of σ^p is inversely related to the energy gap between the relevant occupied and virtual orbitals, with a smaller energy gap leading to a larger chemical shielding. The required mixing may be visualized as rotations of an occupied orbital about one of the three Cartesian axes to produce constructive overlap with an appropriate virtual molecular orbital. Also, Fig. 7 shows that HOMO–LUMO energy gap has the highest

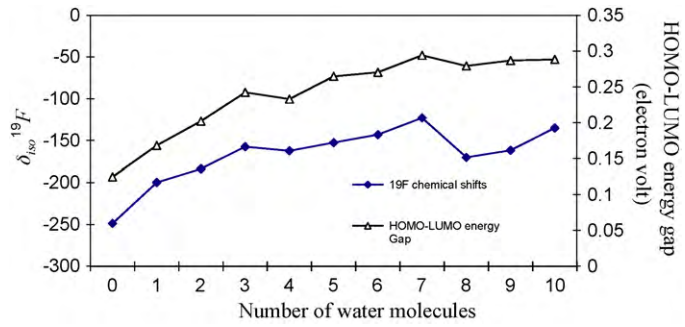

Fig. 7. The variations in ^{19}F NMR chemical shift and HOMO–LUMO energy gap versus the number of water molecules. The chemical shifts obtained from $\delta_{iso} = \sigma_{iso,r} - \sigma_{iso,s}$ $CFCl_3$ with σ_{iso} of 192.7 ppm ^{19}F were chosen as the reference. σ_{iso} obtained by B3LYP/LANL2DZ level at 298.15 K.

value in $n = 7$. Therefore, the hydrated ion-pair with seven hydration numbers is stable.

2.5. Determination of thermodynamic functions

The standard molar thermodynamic functions ΔG^0_m, ΔH^0_m and ΔS^0_m related to the Eq. (1) were determined as follows [41]:

$$\Delta G^0_m = -RT\left(A_1 + \frac{A_2}{DT}\right) \quad (13)$$

$$\Delta S^0_m = R\left[A_1 - \left(\frac{A_2}{D^2}\right)\left(\frac{\partial D}{\partial T}\right)_P\right] \quad (14)$$

$$\Delta H^0_m = -\left(\frac{RA_2}{D}\right)\left[1 + \left(\frac{T}{D}\right)\left(\frac{\partial D}{\partial T}\right)_P\right] \quad (15)$$

The results in various temperatures are listed in Table 1 and can be interpreted by the following equation:

$$Ba^{2+}(H_2O)_x + F^-(H_2O)_y \leftrightarrows [BaF]^+(H_2O)_n + (x + y - n)H_2O \quad (16)$$

In this paper, $x = 6$ and $y = 4$ were used [1]. Table 4 shows the thermodynamic functions of $[BaF]^+$ ion-pair obtained via ab initio method with the various hydration numbers at 25 °C. The hydration number of ion-pair (n) was determined by comparing the results obtained from calculations and experimental data (Table 4) at 25 °C. This comparison supports the results obtained from NMR method, and shows that a good agreement exists between experimental data and DFT calculations in $n = 7$. Therefore,

$$Ba^{2+}(H_2O)_6 + F^-(H_2O)_4 \leftrightarrows [BaF]^+(H_2O)_7 + 3H_2O \quad (17)$$

This process can be viewed as three hypothetical steps: a new bond or interaction is formed between $Ba^{2+}(H_2O)_6$ and $F^-(H_2O)_4$; the

Table 4
Thermodynamic functions (all in kcal/mol) for the reaction of ion-pair formation at 25 °C. The data were obtained by B3LYP/LANL2DZ for $[BaF]^+$ ion-pair in aqueous solution.

n	$[BaF]^+$		
	ΔG^0_m	$T\Delta S^0_m$	ΔH^0_m
0	−82.41	83.20	0.81
1	−72.71	73.69	0.94
2	−60.94	62.04	1.10
3	−50.43	47.92	2.50
4	−40.96	37.77	3.22
5	−31.96	28.68	3.32
6	−20.92	19.38	4.08
7	−5.74	28.75	23.01
8	1.88	29.25	28.62
9	13.69	−8.69	5.04
10	21.14	−15.69	5.44
Exp	−5.15	34.43	29.28

three water molecules are liberated from the hydration spheres; and these liberated water molecules become bound to bulk water. For the first step, the standard molar enthalpy and entropy functions are expected to be negative. For the second step, these functions are both expected to be positive as bond and structure are lost; and for the third step, these functions are expected to be negative. To determine thermodynamic functions via experiment, we carried out experiments at temperatures 25, 30, 35, and 40 °C. The experimental standard molar thermodynamic functions are the sum of the three steps. Table 4 shows that $\Delta S^0_m \succ 0$, $\Delta H^0_m \succ 0$, and $\Delta G^0_m \prec 0$, and that the absolute values increase with increase in temperature. The magnitude of the positive changes in ΔS^0_m would increase if the number of liberated water molecules increases with temperature, or hydrogen bonding decreases. The experimental ΔH^0_m is positive, and varies with temperature. These results show that static electrical interactions are important in ion-pairing. Reardon also arrived at a similar conclusion in the study of the ion-pair $[MgB(OH)_4]^+$ [42]. The experimental ΔG^0_m is negative; therefore, the ion-pairing reaction occurs spontaneously under the conditions of constant temperature and pressure. The Gibbs free energy includes two factors, ΔH^0_m and $T\Delta S^0_m$. The results show that in ion-pairing reaction, ΔH^0_m is less than $T\Delta S^0_m$, and therefore, the entropy of ion-pairing is the dominant thermodynamic factor. The theoretical results also confirm the above results.

3. Conclusion

The subject of ion association was applied to specific case where electrostatic interactions are chemically more significant than structural considerations. The non-ideality of aqueous electrolyte solutions was viewed as having physical (activity coefficient) and chemical (ion-pairing) components, whose contributions depend on the magnitudes of ionic charges, concentrations, and dielectric constants.

In this work, the effect of these factors on thermodynamic values of solubility product and stability constant of formation of ion-pair was investigated both experimentally and theoretically. The NMR results provide an interesting insight into the ion-pairing process in aqueous solution. At finite concentrations, there is a measurable fraction of fluoride ions in solution that exists as the complex. At temperatures near 313.15 K, the separately hydrated Ba^{2+} and F^- ions becomes more stable than $[BaF]^+$ in solution. This observation suggests that the effect of increasing temperature is to decrease the electrostatic attraction of separately hydrated ions to form the ion-pair. DFT calculations show that the minimum energy structure for all the $[BaF]^+(H_2O)_n$ clusters is cyclic. The comparison of the results of NMR and thermodynamic calculations with experimental data show that the seven water molecules hydrated $[BaF]^+$ ion-pair. Also, the HOMO–LUMO energy gap shows that the ion-pair hydrated with seven water molecules is the most stable hydrated ion-pair.

4. Experimental and theoretical sections

4.1. Materials and sample preparation

BaF_2 (suprapure) was purchased from Merck Company and used without further purification. To determine solubility of BaF_2, the saturated solution of BaF_2 was prepared (using deionized and doubly distilled water). The concentration of this solution was determined using gravimetric and solvent evaporation methods ($\sim 7.47 \times 10^{-3}$ M). The solutions of BaF_2 (at different concentrations) were prepared by making stock solution (to 0.00559 M) in 298.15 K. We added to samples a few drops of D_2O, because when chemical shifts were measured, the magnetic field was "locked" to the 2H signal of the heavy water used as a solvent. For the purpose of the line width determination, special attention was paid to optimize the homogeneity of the magnetic field.

4.2. Methods

A Brucker advanced 500 MHz NMR spectrometer was used to obtain ^{19}F NMR spectra at 470.59 MHz and temperatures between 298.15 and 313.15 K.

$CFCl_3$ was used as an external reference to calibrate the chemical shift scale at different temperatures.

The 90°-pulse width was 26.5 μs, and the relaxation delay was 1 s. Typically, signal averaging of 128 scans gave spectra with acceptable signal-to-noise ratios for all samples down 0.0015 M. All shifts were accurate to ±0.1 ppm. Temperature was measured to a precision of ±1 K.

DFT calculations were carried out using the Gaussian 98 suite of programs [43]. Geometry optimization was performed using the DFT calculations with B3LYP level and LANL2DZ basis set [44]. To evaluate the optimized structures for the molecules, frequency calculations were carried out using analytical second derivatives. In all cases, only real frequencies were obtained for the optimized structures.

The Electric Field Gradient (EFG) and chemical shielding tensors of $[BaF]^+$ ion-pair were calculated at level of DFT method including B3LYP with LANL2DZ basis sets for optimized geometry.

The gauge-included atomic orbital (GIAO) approach was used in the chemical shielding tensor calculations [45]. The principal eigenvalues of chemical shielding tensors σ_{11}, σ_{22}, and σ_{33}, were found to have the following relationship:

$$\sigma_{33} > \sigma_{22} > \sigma_{11}$$

Chemical shielding anisotropy ($\Delta\sigma$) was obtained by $\Delta\sigma = \sigma_{33} - (\sigma_{22} + \sigma_{11})/2$, and chemical shielding isotropy (σ_{iso}) was obtained by $\sigma_{iso} = (\sigma_{11} + \sigma_{22} + \sigma_{33})/3$. To convert $\sigma_{iso}(^{19}F)$ to chemical shift isotropy, δ_{iso}, $CFCl_3$ ($\sigma_{iso}(^{19}F) = 192.7$ ppm) was chosen as the reference, $\delta_{iso} = \sigma_{iso,r} - \sigma_{iso,s}$, where the subscripts "r" and "s" refer to the reference and sample, respectively [46,47].

The principal eigenvalues for EFG tensors q_{xx}, q_{yy} and q_{zz} have the following relationship:

$$|q_{zz}| \geq |q_{yy}| \geq |q_{xx}|$$

The nuclear quadrupole coupling constant (χ) was obtained by: $\chi(\text{MHz}) = e^2 Q q_{zz}/h$ where "e" is the charge of electron, Q is the nuclear electric quadrupole moment, and "h" is the Planck's constant. Q value for ^{135}Ba used in the calculation of χ value has been reported by Pyykko to be 1.6×10^{-31} m^2 [48].

Another important parameter which refers to the deviation of charge distribution from cylindrical symmetry is the asymmetry parameter (η) obtained by:

$$\eta = \left| \frac{q_{yy} - q_{xx}}{q_{zz}} \right|.$$

Appendix A. Nomenclature

a'	the distance of the closest approach between two ions
a	the activity of solution
D	dielectric constant
e	the elementary charge
$f_\pm$	mean activity coefficient
f_i	activity coefficient of ionic species
K	stability constant of formation of ion-pair
k	the Boltzmann constant
M	the concentration of solution
N	Avogadro's number

n hydration number
Q the nuclear electric quadrupole moment
q EFG tensor eigenvalue
R gas constant
T absolute temperature
χ quadrupole coupling constant
Z the number of electrical charge
α the fraction of the total F^- free ions in solution
δ chemical shift
σ chemical shielding
η asymmetry parameter
τ mean life time

Appendix B

For formation of ion-pair,

$$Ba^{2+} + F^- \leftrightarrows [BaF]^+ : \quad K = \frac{a_{[BaF]^+}}{a_{Ba^{2+}} a_{F^-}} \tag{B-1}$$

$$K = \frac{[BaF]^+}{[Ba^{2+}][F^-]} \times \frac{f_{ion\text{-}pair}}{f_+ f_-} \tag{B-2}$$

where $[i]$ and f_i are molar concentration and activity coefficient for i species in solution, respectively.

$\log K$ is written as follows:

$$\log K = \log K' + \log f_{ion\text{-}pair} - \log f_+ - \log f_- \tag{B-3}$$

where K' is concentration equilibrium constant and $\log f_i = -(AZ_i^2\sqrt{I}/(1 + Ba'\sqrt{I})) + bI$.

Therefore,

$$\log K = \log K' - \frac{A\sqrt{I}}{1 + Ba'\sqrt{I}} + bI + \frac{4A\sqrt{I}}{1 + Ba'\sqrt{I}} - bI + \frac{A\sqrt{I}}{1 + Ba'\sqrt{I}} - bI \tag{B-4}$$

$$\log K = m - bI \tag{B-5}$$

where $m = \log K' + (4A\sqrt{I}/(1 + Ba'\sqrt{I}))$ and b is an empirical parameter.

When the plot of y versus x for $y = \boldsymbol{\alpha} + \boldsymbol{\beta}x$ did not have a clear slope, then least-square method was used to determine intercept and slope.

Appendix C. Supplementary data

Supplementary data associated with this article can be found, in the online version, at doi:10.1016/j.jfluchem.2010.07.001.

References

[1] J.óM. Bockris, A.K.N. Reddy, second ed., Modern Electrochemistry, vol. 1, Plenum Press, New York/London, 1998.
[2] B.E. Conway, Ionic Hydration in Chemistry and Biophysics, Elsevier, Amsterdam, 1981.
[3] C. Reichardt, Solvent Effects in Organic Chemistry, Verlag Chemie, Weinheim, 1979.
[4] M. Nakahara, in: H. Ohtaki, H. Yamatera (Eds.), Structure and Dynamics of Solutions, Elsevier, Amsterdam, 1992.
[5] E. Leontidis, Curr. Opin. Colloid Interface Sci. 7 (2002) 81–91.
[6] A.K. Soper, K. Weckström, Biophys. Chem. 124 (2006) 180–191.
[7] B. Hribar, N.T. Southall, V. Vlachy, K.A. Dill, J. Am. Chem. Soc. 124 (2002) 12302–12311.
[8] Y. Marcus, Ion Solvation, Wiley, London, 1985.
[9] P. Turq, L. Blum, O. Bernard, W. Kunz, J. Phys. Chem. 99 (1995) 822–827.
[10] O. Bernard, W. Kunz, P. Turq, L. Blum, J. Phys. Chem. 96 (1992) 3833–3840.
[11] W.H. Lee, R.J. Wheaton, J. Chem. Soc., Faraday Trans. 2 74 (1978) 743–766; W.H. Lee, R.J. Wheaton, J. Chem. Soc., Faraday Trans. 2 74 (1978) 1456–1482; W.H. Lee, R.J. Wheaton, J. Chem. Soc., Faraday Trans. 2 75 (1979) 1128–1145.
[12] H. Krienke, J. Barthel, J. Mol. Liquids 78 (1998) 123–138.
[13] H. Bianchi, H.R. Corti, R. Fernandez-Prini, J. Solut. Chem. 17 (1988) 1059–1065.
[14] K. Indaratna, A.J. Mcquillan, R.A. Matheson, J. Chem. Soc., Faraday Trans. 1 82 (1986) 2755–2762.
[15] A.V. Sharygin, I. Mokbel, C. Xiao, R.H. Wood, J. Phys. Chem. B 105 (2001) 229–237.
[16] S.G. Capewell, G.T. Hefter, P.M. May, Talanta 49 (1999) 25–30.
[17] S.O. Russo, G.I.H. Hanania, J. Chem. Educ. 66 (1989) 148–153.
[18] N. Altounian, A. Glatfelter, S. Bai, C. Dybowski, J. Phys. Chem. B 104 (2000) 4723–4725.
[19] D.P. Bossev, M. Matsumoto, M. Nakahara, J. Phys. Chem. B 103 (1999) 8251–8258.
[20] D.P. Bossev, M. Matsumoto, T. Sato, H. Watanabe, M. Nakahara, J. Phys. Chem. B 103 (1999) 8259–8266.
[21] W.H. Otto, D.J. Britten, C.K. Larive, J. Colloid Interface Sci. 261 (2003) 508–513.
[22] I.M. Ward, N. Boden, J. Cruickshank, S.A. Leng, Electrochim. Acta 40 (1995) 2071–2076.
[23] A. Mizoguchi, Y. Ohshima, Y. Endo, J. Am. Chem. Soc. 125 (2003) 1716–1717.
[24] D.E. Woon, T.H. Dunning Jr., J. Am. Chem. Soc. 117 (1995) 1090–1097.
[25] M. Pavlov, P.E.M. Siegbahn, M. Sandström, J. Phys. Chem. A 102 (1998) 219–228.
[26] T. Megyes, I. Bakó, S. Bálint, T. Grósz, T. Radnai, J. Mol. Liquids 129 (2006) 63–74.
[27] A. Tongraar, B.M. Rode, Chem. Phys. Lett. 409 (2005) 304–309.
[28] H. Fukaya, T. Ono, J. Comput. Chem. 2 (2003) 551–560.
[29] M. Lia, Z. Duan, Z. Zhang, C. Zhang, J. Weare, Mol. Phys. 106 (2008) 2685–2697.
[30] F. Jalilehvand, D. Spangberg, P. Lindqvist-Reis, K. Hermansson, I. Persson, M. Sandstrom, J. Am. Chem. Soc. 123 (2001) 431–441.
[31] T.C. Franklin, V. Totten, A. Aktan, J. Electrochem. Soc. 135 (1988) 1638–1640.
[32] G. Makov, A. Nitzan, J. Phys. Chem. 96 (1992) 2965–2967.
[33] J.L. Kaplan, G. Fraenkel, NMR of Chemically Exchanging Systems, Academic Press, New York, 1980.
[34] G.E. Maciel, L. Simeral, J.J.H. Ackerman, J. Phys. Chem. 81 (1977) 263–267.
[35] J. Burgess, Ions in Solution: Basic Principles of Chemical Interactions, John Wiley & Sons, New York, 1988.
[36] S.P. Tanner, J.B. Walker, G.R. Choppin, J. Inorg. Nucl. Chem. 30 (1968) 2067–2070.
[37] V. Majer, K. Štulík, Talanta 29 (1982) 145–148.
[38] P. Stilbs, Prog. NMR Spectrosc. 19 (1987) 1–45.
[39] N.F. Ramsey, Phys. Rev. 77 (1950) 567–575.
[40] N.F. Ramsey, Phys. Rev. 86 (1952) 243–246.
[41] J.Z. Yang, R.B. Zhang, H. Xue, P. Tian, J. Chem. Thermodyn. 34 (2002) 401–407.
[42] E.J. Reardon, Chem. Geol. 18 (1976) 309–325.
[43] M.J. Frisch, G.W. Trucks, H.B. Schlegel, G.E. Scuseria, M.A. Robb, J.R. Cheeseman, V.G. Zakrzewski, J.A. Montgomery Jr., R.E. Stramann, J.C. Burant, S. Dapprich, J.M. Millam, A.D. Daniels, K.N. Kudin, M.C. Strain, O. Farkas, J. Tomasi, V. Barone, M. Cossi, R. Commi, B. Mennucci, C. Pomelli, C. Adamo, S. Cliffod, J. Ochterski, G.A. Peterson, P.Y. Ayaly, Q. Cui, K. Morokuma, D.K. Malick, A.D. Rabuck, K. Raghavachari, J.B. Foresman, J. Ciolowski, J.V. Oriz, B.B. Stefanov, G. Liu, A. Liashenko, P. Piskorz, I. Komaromi, R. Gomperts, R.L. Martin, D.J. Fox, T. Keith, M.A. Al-Laham, C.Y. Peng, A. Nanayakkara, C. Gonzalez, M. Challacomb, P.M.W. Gill, B. Johnson, W. Chen, M.W. Wong, J.L. Andres, C. Gonzales, M. Head-Gordon, E.S. Replogle, J.A. Pople, Gaussian 98, Gaussian, Inc., Pittsburg, PA, 1998.
[44] W. Yang, R.G. Parr, Density-functional Theory of Atoms and Molecules, Oxford University Press, Oxford, 1989.
[45] K. Wolinski, J.F. Hinton, P. Pulay, J. Am. Chem. Soc. 112 (1990) 8251–8260.
[46] A. Antušek, K. Jackowski, M. Jaszuński, W. Makulski, M. Wilczek, Chem. Phys. Lett. 411 (2005) 111–116.
[47] K. Jackowski, M. Kubiszewski, W. Makulski, J. Mol. Struct. 614 (2002) 267–272.
[48] P. Pyykkö, Mol. Phys. 99 (2001) 1617–1629.